Elastic Membrane. Formulation and Validation.

1 Formulation

Governing equations for a fluid flow with elastic membrane model are incompressible Navier-Stokes equations

$$u_{i,\,t} + u_j\,u_{i,\,j} = \tau_{ij,j} + f_i \quad (1)$$

$$u_{i,\,i} = 0, \quad (2)$$

where the stress tensor is defined by

$$\tau_{ij} = -\frac{P}{\rho} + \nu(u_{i,\,j} + u_{j,\,i}). \quad (3)$$

Boundary conditions on the elastic membrane are formulated as follows:

$$\sigma_n - p_e = -\sigma k T \quad (4)$$

$$\mathbf{u} = \mathbf{w} \quad (5)$$

The first condition is the traction boundary condition, with σ_n – the normal fluid stress acting on the membrane, p_e – external pressure, T – the longitudinal tension and k – the wall curvature. The second condition is the kinematic condition, where $\mathbf{w}$ is the wall velocity. The details of the implementation can be found in Ref. [1].

2 2D validation

2.1 Steady case

For validation in two dimensions we simulate a steady flow in a two-dimensional channel with the bottom solid wall and top wall being a combination of solid and elastic sections [2]. All geometrical and physical parameters are taken from the Ref. [2], namely, $p_e = 0.93\,Pa$, $Re = 300$, $T = T_0/\beta$, $T_0 = 1.610245\,N\,m^{-1}$, β is ranging from 1 to 30. For every Reynolds number, there exists a critical surface tension $T^\star$, such that solutions are stable for $T > T^\star$, and they become unstable for $T \leq T^\star$. In terms of the parameter β, solutions are stable for $\beta < \beta^\star$, and unstable for $\beta \geq \beta^\star$. Dependence of the critical parameter $\beta^\star$ on the Reynolds number is illustrated in Fig. 1 for our calculations and for the calculations of Luo & Pedley[3]. Exact values of the critical parameter $\beta^\star$ are summarized in Table 1. It is seen that the results are very close (within the error bars $Err(\beta^\star) = \pm 1$). The parameter space below the neutral stability curve correspond to stable solutions, and above the curve - to unstable solutions. With the unsteady solver, steady solutions can not be obtained for $\beta \geq \beta^\star$ due to

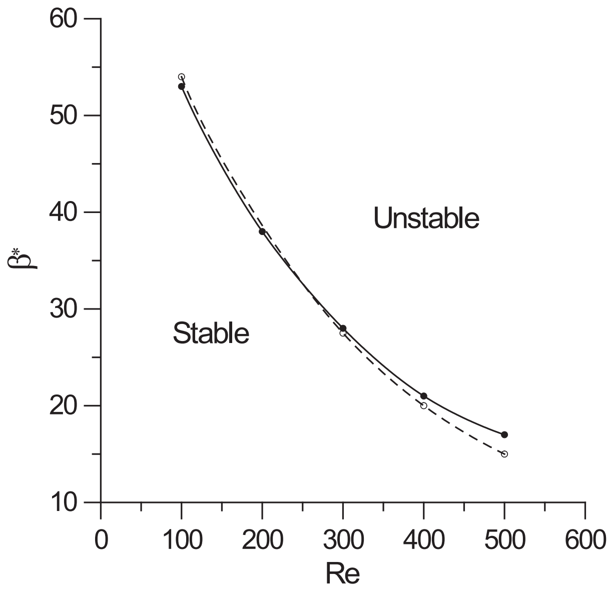

Figure 1: Dependence of the critical parameter $\beta^\star$ on Reynolds number. Filled circles and the solid line, current simulations; open circles and the dashed line, simulations of Luo&Peldey [3]

Table 1: Dependence of the critical parameter $\beta^\star$ on Reynolds number

Reynolds number	$Re = 100$	$Re = 200$	$Re = 300$	$Re = 400$	$Re = 500$
Current calculations	53	38	28	21	17
Luo&Pedley [3]	54	–	27.5	20	15

the instability. We have performed grid refinement study for stable solutions for $\beta = 20$ at two different Reynolds numbers, $Re = 300$ and $Re = 400$. Number of collocation points within the elements was varied from $l = 5$ to $l = 7$. Differences were insignificant between $l = 6$ and $l = 7$ solutions, see Fig. 3, so we consider solutions with $l = 6$ to be spatially converged. Comparison of the wall shape and the pressure drop with the simulations of Luo & Pedley [2] for $Re = 300$ and $Re = 400$, $\beta = 20$, with $l = 6$ is shown in Fig. 4.

2.2 Unsteady case

When the tension T falls below the critical tension $T^\star$ (or parameter β exceeds $\beta^\star$), the solution is unstable to small perturbations. We have computed the unstable case with $Re = 300$ and $\beta = 30$ following the article of Luo&Peldey [3] ($\beta^\star \sim 28$ for this Reynolds number). We have found that the temporal behavior depends on initial conditions, see Fig. 6, where three different initial conditions for $Re = 300$ were used: plane channel flow, steady solution corresponding to $\beta = 25$, and steady solution corresponding to $\beta = 27.5$ (the highest β for which

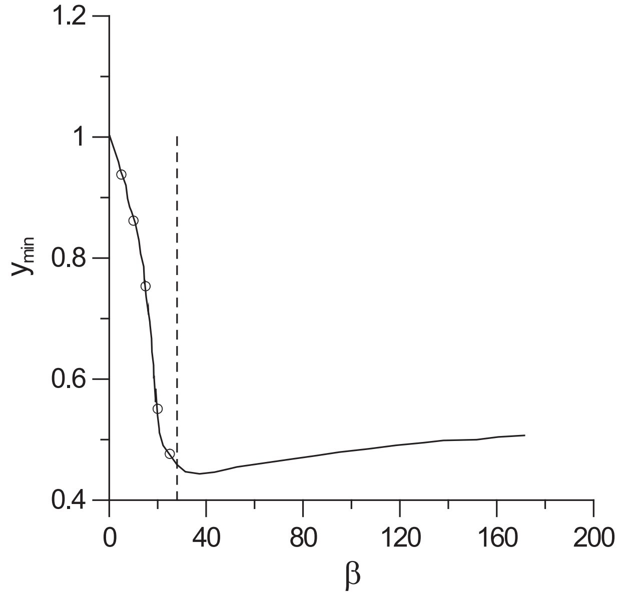

Figure 2: Dependence of y_{min} versus β, $Re = 300$. Line, simulations of Luo & Pedley [2], symbols - current simulations, vertical dashed line signifies the critical tension, $\beta = 28$, so that steady solutions are not available for $\beta > 28$.

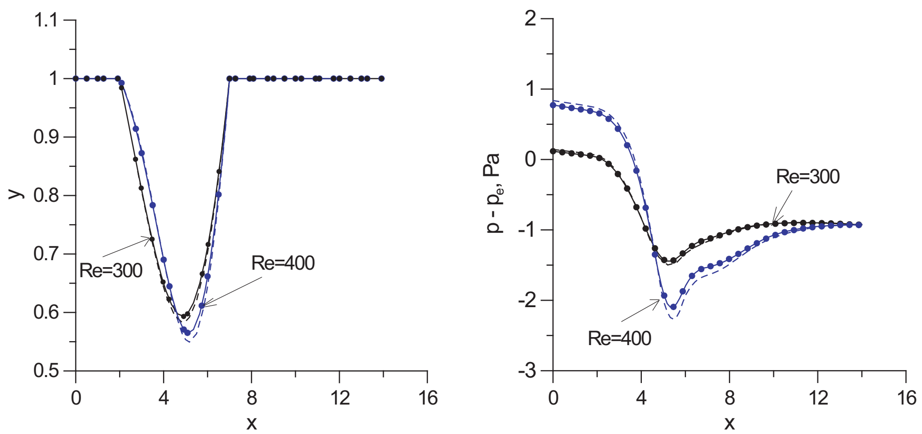

(a) Wall shape

(b) Pressure drop

Figure 3: Grid refinement study. $\beta = 20$, $Re = 300$ and $Re = 400$. Dashed line, $l = 5$; solid line, $l = 6$; symbols, $l = 7$ (every 3rd grid point is shown).

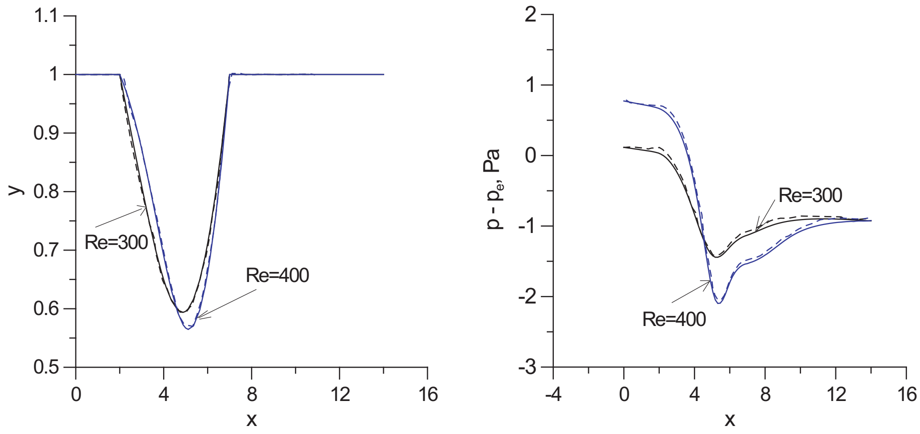

(a) Wall shape

(b) Pressure drop

Figure 4: Comparison with the simulations of Luo & Pedley[2] at $\beta = 20$, $Re = 300$ and $Re = 400$. Solid line, current simulations; dashed line, simulations of Luo & Pedley [2].

we were able to obtain a steady solution for this Reynolds number). Fig. 6 shows the wall position y_w at $x_w = 8.5$ versus time. It is seen that all three cases reach the periodic state, but the system response is completely different. When the initial conditions ($\beta = 27.5$) are close to the current value of tension ($\beta = 30$), the perturbations are small enough, so that the system responds in a linear regime, close to a simple harmonic. When the initial conditions are further from the current state ($\beta = 25$ versus $\beta = 30$), the non-linear effects are more pronounced, and the second frequency is activated. When initial conditions are very far from the current state (channel flow corresponding to a solid wall with $\beta = 0$), the response is highly-nonlinear. This trend was also observed at other values of Reynolds number, as well as in the Ref. [3]. Due to the extreme sensitivity of the system behavior to initial conditions, it is quite difficult to compare the temporal behavior with the previously published results. Luo&Pedley [3] calculated the case with $Re = 300$ and $\beta = 30$ by imposing a small disturbance on the steady solution, disturbance being a slightly different value of initial tension. Comparison of our calculations with initial $\beta = 27.5$, which is the closest steady solution to $\beta = 30$ which we could obtain, with the calculations of Luo&Pedley [3] is shown in Fig. 7, where the wall position y_w and wall pressure p_w at $x_w = 8.5$ are plotted. It is seen that the agreement is fairly good, with amplitudes for both the wall position and pressure matching well. Our frequency ($f \sim 0.07$ Hz) is a little bit lower than the frequency observed in Luo&Pedley ($f \sim 0.1$ Hz). To understand the reason for the difference in frequency, we have calculated frequencies of linear harmonic response for $\beta = \beta^\star$ at different Re, since steady solutions with the tension very close to $T^\star$ can be obtained as initial conditions to provide the linear response. The dependence

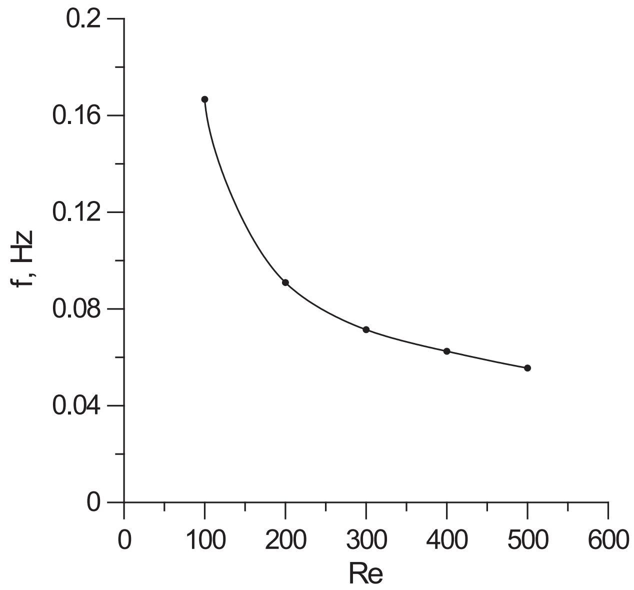

Figure 5: Dependence of the linear response frequency on Reynolds number. Symbols, calculated frequencies; line, spline fit.

Table 2: Dependence of the linear response frequency on Reynolds number

Reynolds number	$Re = 100$	$Re = 200$	$Re = 300$	$Re = 400$	$Re = 500$
Frequency, Hz	0.16	0.09	0.07	0.06	0.05

on Reynolds number is shown in Fig. 5 and tabulated in Table 2. The trend is that the frequency decreases with the Reynolds number. Thus, larger frequency in calculations of Luo&Pedley [3] might signify the larger amount of dissipation in their finite element code versus the low-dissipation spectral element method.

References

[1] L.-W. Ho. *A Legendre spectral element method for simulation of incompressible unsteady viscous free-surface flows.* PhD thesis, Massachusetts Institute of Technology, 1989.

[2] X. Y Luo and T J. Pedley. A numerical simulation of steady flow in a 2-D collapsible chnnel. *J. Fluids Struct.*, 9:149–174, 1995.

[3] X. Y Luo and T J. Pedley. A numerical simulation of unsteady flow in a two-dimensional collapsible chnnel. *J. Fluid Mech.*, 314:191–225, 1996.

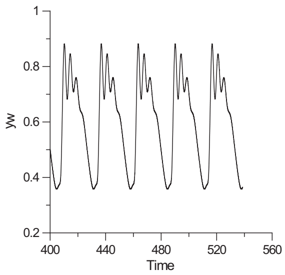

(a) Initial conditions correspond to flow with a solid wall ($\beta = 0$)

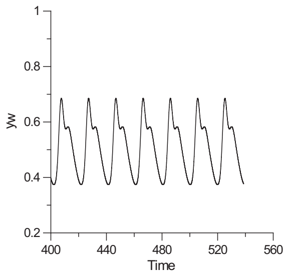

(b) Initial conditions correspond to steady flow with $\beta = 25$

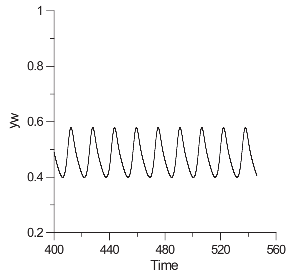

(c) Initial conditions correspond to steady flow with $\beta = 27.5$

Figure 6: Influence of initial conditions on temporal behavior of unsteady solutions. $Re = 300$, $\beta = 30$.

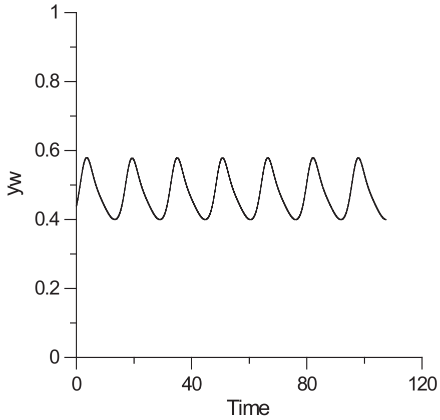

(a) Wall position

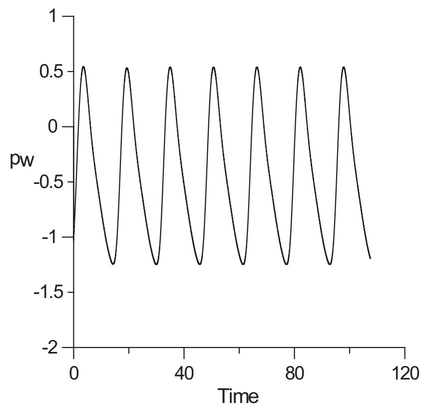

(b) Pressure

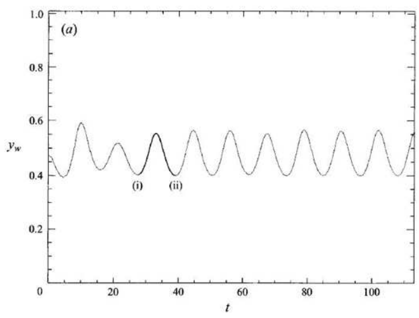

(c) Wall position

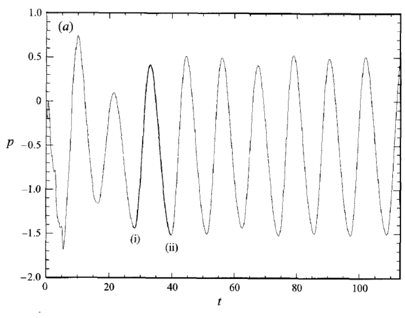

(d) Pressure

Figure 7: Comparison of temporal behavior with calculations of Luo&Pedley. Wall position y_w and pressure at $x_w = 8.5$ versus time is plotted. Top row - current calculations, bottom row - calculations of Luo&Pedley [3]